Bull Volcanol (2016) 78:69
DOI 10.1007/s00445-016-1063-y

RESEARCH ARTICLE

Short-lived eruptive episodes during the construction of a Na-alkalic basaltic field (Perşani Mountains, SE Transylvania, Romania)

Ioan Seghedi[1] · Răzvan-Gabriel Popa[2,1] · Cristian G. Panaiotu[3] · Alexandru Szakács[4,1] · Zoltán Pécskay[5]

Received: 31 December 2015 / Accepted: 5 September 2016

Abstract The Perşani Mts. basaltic field covers >176 km^2 (~22 × 8 km) and is one of the youngest and biggest monogenetic volcanic fields in Southeastern Europe. It consists of 21 monogenetic volcanic centers, most of which were built on a basement of Miocene rhyolitic tuffs and Mesozoic sedimentary rocks. $^{40}Ar/^{39}Ar$ dating shows that the eruptions took place in five episodes: 1220, 1142, 1060, 800, and 683 ka. An additional undated episode at 1060–800 ka has been identified using volcanological observations. Initial phreatomagmatic activity was commonly followed by explosive Strombolian/Hawaiian phases that deposited agglutinated spatter around the vents along with massive-to-bedded unconsolidated scoria and lapilli. Some volcanoes lack evidence for magmatic explosive activity, while others lack evidence for the initial phreatomagmatic phase. During most eruptions, the final activity was the effusion of lava flows that in some cases deformed (or partially destroyed) the volcanic edifices. The erupted volumes varied greatly from one episode to other, without showing any pattern: the highest volumes are recorded in deposits from the third pulse (1060 ka). The volcanoes are located close to faults and always on their footwall blocks, and it is inferred that the regional tectonic stress regime controlled both the timing and spacing of volcanic activity in the volcanic field.

Keywords Perşani Mountains · Monogenetic Na-alkalic volcanoes · Phreatomagmatic · Tectonic control

Editorial responsibility: R.J. Brown

Electronic supplementary material The online version of this article (doi:10.1007/s00445-016-1063-y) contains supplementary material, which is available to authorized users.

✉ Ioan Seghedi
seghedi@geodin.ro

1 Institute of Geodynamics, Romanian Academy, 19-21 Jean Louis Calderon, Bucharest, Romania

2 Institute of Geochemistry and Petrology, ETH Zürich, Clausiusstrasse, 25 Zürich, NO, Switzerland

3 Paleomagnetic Laboratory, University of Bucharest, Bălcescu 1, 010041 Bucharest, Romania

4 Department of Environmental Sciences, Sapientia University, 4 Matei Corvin Str, RO-400112 Cluj-Napoca, Romania

5 Institute of Nuclear Research of Hungarian Academy of Sciences, Bem tér 18/c, Debrecen 4026, Hungary

Introduction

The Perşani Mountains Volcanic Field (PMVF) is located in the internal part of the Carpathian Bend Area and intersects the Olt valley ca. 40 km NW of the city of Braşov, in the southeastern corner of the Transylvanian Basin (Fig. 1). It was initially studied in the late nineteenth and early twentieth century (Hauer and Stache 1863; Herbich 1878); Koch 1900; Wachner 1915; Laţiu 1928). The first volcanological reconstructions were attempted by Preda (1940), Mihăilă et al. (1972), and Mihăilă and Peltz (1977). Seghedi and Szakács (1994) conducted the first systematic approach, but the evolution of the PMVF is now much better constrained by paleomagnetic, K–Ar (Ghenea et al. 1981; Mihăilă and Kreutzer 1981; Panaiotu et al. 2004), and $^{40}Ar/^{39}Ar$ dating methods (Panaiotu et al. 2013). New paleomagnetic data (Panaiotu et al. 2016) have helped refine volcanological reconstructions.

Monogenetic volcanoes are common worldwide and develop in a single eruptive event lasting weeks to decades (i.e., Connor and Conway 2000). They are usually of small volume (~1 km^3) and comprise a great variety of edifice styles, such as scoria cones, maars, tuff rings, and tuff cones (e.g., Valentine and Gregg 2008; Kereszturi and Németh 2012). Recent

Published online: 15 September 2016

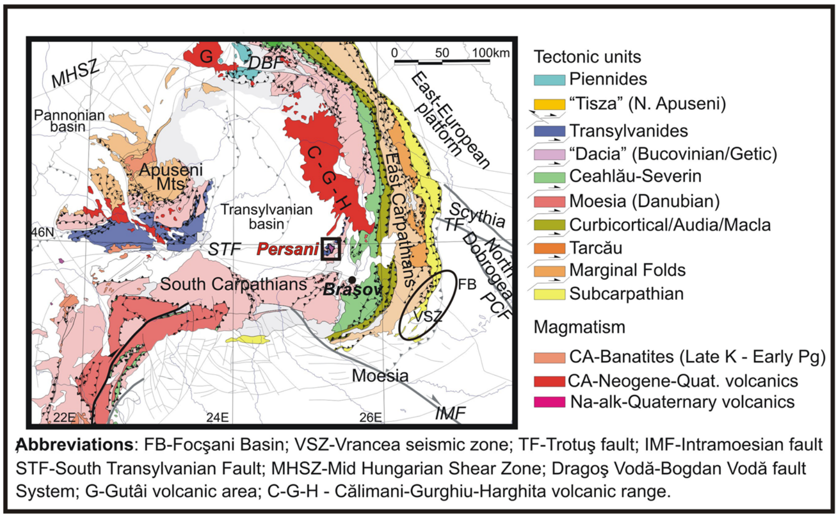

Fig. 1 Location of the PMVF within the tectonic map of the Romanian Carpathians (compiled from Matenco et al. 2010; Săndulescu 1984; Schmid et al. 2008)

developments in the study of these types of volcanoes added important information to the understanding of fundamental processes of basaltic volcanism, its generation, and relationships with regional geodynamic processes and tectonic setting (e.g., Le Corvec et al. 2013). Long-term evolution in tectonically controlled volcanic fields is likely to be time-predictable (duration of repose period is proportional to the volume of the preceding eruption) favored by pre-existing faults and occasionally volume-predictable (volume of next eruption depends upon the duration of repose leading up to it) (e.g., Gaffney et al. 2007; Valentine and Perry 2007). The most important achievements include (i) the detection of short- and long-term changes occurring during emplacement of a single vent and/or a volcanic field (e.g., Kereszturi and Németh 2012), (ii) evidence of the evolution of magmatic systems of individual small-volume volcanoes (e.g., Harangi et al. 2013), (iii) a better understanding of eruption mechanisms, edifice growth, and hazards of monogenetic volcanism based on observation of the internal architecture of a volcano (e.g., Marti et al. 2011; Cimarelli et al. 2013), (iv) the relationship between magma feeding system (dominantly dykes) and local and regional tectonic factors (Tibaldi and Mariotto 2015), etc.

Recent research in the Carpathian-Pannonian Region (CPR), in particular, has advanced the knowledge regarding the development and eruption styles of monogenetic volcanism in the area (e.g., Németh and Martin 1999, 2007; Martin and Németh 2004; Lexa et al. 2010), contributing to the understanding of monogenetic volcanism in general and of its relationships with regional and local tectonic features.

In such a general and regional context, the renewed and detailed investigation of the Na-alkaline PMVF is relevant for a number of reasons: (i) it represents the easternmost (i.e., peripheral) occurrence of monogenetic volcanism in the CPR; (ii) it contributes to a better understanding of mantle processes operating in the whole CPR in the Neogene-Quaternary time interval, by providing new data that can be correlated to other fields in the area (e.g., the Nógrád-Novograd and Bakony-Balaton Highland monogenetic volcanic fields, Németh 2012; Kereszturi et al. 2011); (iii) it helps improve understanding of the ongoing geodynamics of the Carpathian bend area; and (iv) it adds value to an initiative for a Perşani Geopark.

Here, we investigate the relationships between eruption style, timing, volcano distribution, and local tectonics, based on a detailed volcanological analysis and on geological mapping combined with paleomagnetic and recent radiometric age data. Volcano morphology derived from field data and digital elevation models (DEM) helps to discriminate among the different types of eroded volcanic structures. The volumes of scoria cones and lava fields are also estimated based on DEMs. Overall, this study attempts a new volcano-structural analysis to better understand the timing, style, and "triggering factors" of the volcanic activity in the studied area, clarifying on the evolution of magma plumbing systems in relationship to the tectonic regime during volcanism.

Regional geologic background

The anorogenic mafic Na-alkalic volcanism of the PMVF was contemporaneous with orogenic adakite-like calc-alkaline volcanism of the southernmost Harghita Mountains, located 40 km to the east (Fig. 1; Szakács et al. 1993; Seghedi et al. 2004, 2011). The calc-alkaline magmatism of the South Harghita Mts. developed from corner flow around a steepening slab (Vrancea slab below Moesia platform) (Seghedi et al. 2011), whereas the K-alkalic magmatism of the South Harghita Mts. and the Perşani Na-alkalic magmatism are considered to have been triggered by asthenosphere ascent during slab steepening (Seghedi et al. 2011; Harangi et al. 2013). Thus, three contemporaneous magma sources (Na-alkalic, K-alkalic, and adakite-like calc-alkaline) are present in a small area. It seems that the ascent of magmas was facilitated by the same regional tectonic event, coeval with the last episode (latest Pliocene onward) of tectonic inversion in the Southeastern Carpathians (Matenco et al. 2007; Seghedi et al. 2011).

The PMVF is the youngest (1.2–0.6 Ma) Na-alkalic basaltic volcanism in Eastern Europe (Panaiotu et al. 2013). It consists of volcanoes with variable morphologies (from cone- to crater-shaped), which are a result of the dominant eruptive style that typically evolved from phreatomagmatic to Strombolian and effusive phases. There is a central zone of 14 volcanoes and two peripheral zones, with sparsely distributed volcanoes (Fig. 2).

The common occurrence of mantle xenoliths in the Perşani volcanic deposits (e.g., Vaselli et al. 1995; Falus et al. 2008) provides evidence of rapid magma ascent. Petrological data also suggest high ascent rates: the basaltic magmas traversed the crust within only 4–5 days (Harangi et al. 2013). This, along with the practically homogeneous geochemical composition during the time-span of volcanic activity, indicates that the magmas were generated by deep mantle processes and were mostly unaffected by the interaction with the crust (Downes et al. 1995). The petrological aspects of PMVF basalts are similar to continental intraplate alkali basalts worldwide (Lustrino and Wilson 2007; Harangi et al. 2014). They also show some subtle features (e.g., Pb isotopic characteristics, high LILE) resembling those of subduction-related magmas, suggesting generation from a mantle source slightly influenced by subduction components (Downes et al. 1995; Seghedi et al. 2011; Harangi et al. 2013).

The Perşani Mountains Volcanic Field—general features

The PMVF comprises 21 volcanoes (Fig. 2). Five of them, namely Fântâna, Gruiu-Mic, Dîlma-West, Trestia-South, and Comana-South are documented here for the first time.

There is one large volcanic cluster consisting of nine volcanoes (Măguricea, Bârc, Fântâna, 636, Bogata, Dîlma-West, Pietrele, Gruiu, and Gruiu-Mic) developed in four episodes. All the other volcanoes are isolated from each other (their deposits do not overlap).

The volcaniclastic terminology used in this paper to describe the deposits follows Fisher and Schmincke (1984) and White and Houghton (2006). Three main styles of volcanic activity are recorded (Seghedi and Szakács 1994), namely: phreatomagmatic, Strombolian, and effusive. Tectonic analysis was also considered.

Phreatomagmatic explosive activity

Phreatomagmatic activity generated maars and tuff rings. The phreatomagmatic successions (Fig. 3) typically involve low-angle alternating tuff and lapilli-tuff beds rich in accidental lithic clasts and displaying either plane-parallel stratification or cross-lamination. Bomb sags from ballistically emplaced basement clasts are common in proximal facies. Mantle xenoliths and amphibole xenocrysts are common and are most abundant in the deposits of the Bârc and Fântâna volcanoes. The thickest and most complex sequence of phreatomagmatic deposits outcrops on the left bank of Trestia valley and belongs to the eroded outer parts of the Bârc volcano.

Most of the phreatomagmatic edifices are eroded, and quantitative parameters such as crater depth and crater floor diameter cannot be estimated. The crater upper diameter can be approximated and, according to this parameter, the widest is Bârc (~2.25 km) with Bogata volcano having the second widest crater (0.9 km); however, the crater rim is enlarged due to erosion.

Syn-eruptive degradation due to erosional crater enlargement or subhorizontal sill injection at the base of tuff rings is inferred. This has occurred at Racoş and Bogata where the horizontal intrusions have laterally feed lava flows. Sometimes lava flows breached the edifices and caused their partial collapse (Turzun, Bârc, 636, Dîlma-West, Pietrele volcanoes). At the Măguricea volcano, the initial volcanic structure (tuff ring or maar) was completely destroyed by later effusive activity; its existence can be inferred from blocks of phreatomagmatic deposits that were rafted by the lava flows. For most volcanoes, the relative position of the crater floor with respect to the bedrock (and pre-volcanic topography) can only be estimated.

Strombolian/Hawaiian explosive activity

The Strombolian and Hawaiian explosive eruption styles both occur in low-viscosity systems and are influenced by two end-member flow types (annular and slug flow) that are part of a continuum (Vergnoille and Mangan 2000). Their deposits are sometimes difficult to distinguish. Evidence for typical Hawaiian-type activity is given by the presence in some volcanoes of near-vent spatter and agglutinated products, such as at the scoria cone of the Racoş volcano, where a fountain-related rootless lava flow is visible in a quarry. These deposits are surrounded by unconsolidated lapilli tuffs typical of Strombolian origin. At all other scoria cones, the preserved pyroclastic deposits do not show any diagnostic features of Hawaiian activity. Hence, we infer that Strombolian activity was dominant during the eruptions in the PMVF. Strombolian with possibly minor Hawaiian activity generated 17 scoria cones.

All cones are affected to varying degrees by both syn-eruptive and post-eruptive erosion. The cone of Turzun volcano has been completely destroyed by vertical fault movements. Syn-eruptive cone degradation resulted from lava flows either flowing from the base of the cones (e.g.,

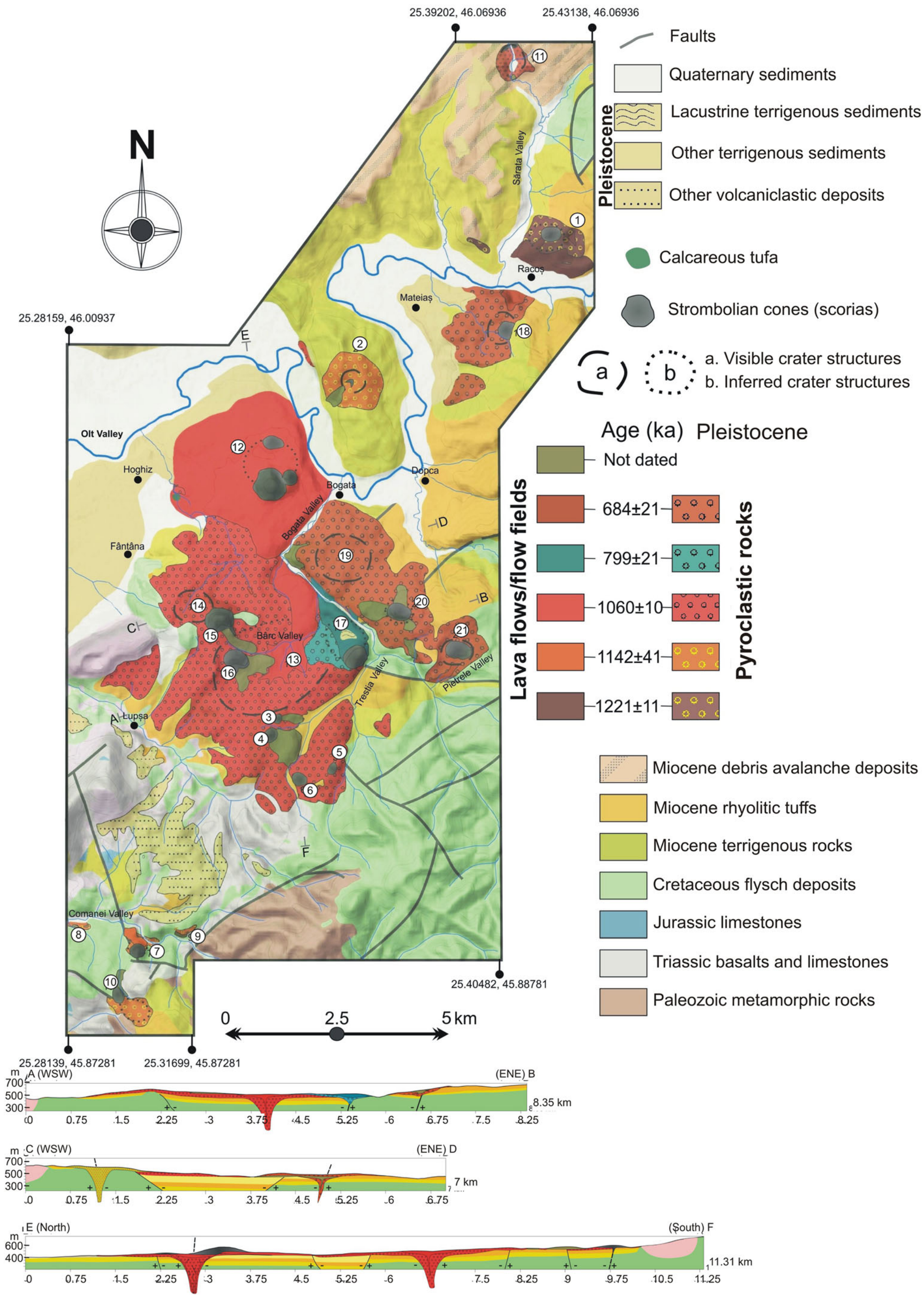

Fig. 2 The new volcanological map of the PMVF. This map is the result of field mapping and data compilation (Popescu 1970; Popescu et al. 1976; Seghedi and Szakács 1994). The *numbers on the map* denote individual volcanic structures: *1*, Racoş; *2*, Turzun; *3*, Trestia-Nord; *4*, Trestia-West; *5*, Trestia-East; *6*, Trestia-South; *7*, Comana; *8*, Comana-West; *9*, Comana-East; *10*, Comana-South; *11*, Sărata; *12*, Măguricea; *13*, Bârc; *14*, Fântâna; *15*, Gruiu; *16*, Gruiu-Mic; *17*, 636 (since all nearby topographic names were already committed to other volcanoes, we named this one after the altitude of its peak); *18*, Mateiaş; *19*, Bogata; *20*, Dîlma-West; *21*, Pietrele. Coordinates are given in the WGS84 reference system and are placed at the corners of the map

Măguricea volcano) or breaching them (e.g., the Gruiu, Gruiu-Mic, and 636 volcano).

The internal structure of a scoria cone is best exposed by quarrying at Racoş volcano (Fig. 4a–c). Its center consists of a massive spatter deposit welded to various degrees and of remnants of thin clastogenic lava tongues. Basaltic bombs up to 100 cm in diameter are common. Agglutinated spatter beds are intercalated with coarse-grained spatter layers showing cross-cutting relationships, suggesting pulsating eruptions. The grain size of the scoria deposits decreases considerably in the marginal facies of the cone, which are dominantly composed of massive and layered unconsolidated coarse ash and lapilli-tuff fall deposits.

The remaining scoria cones (Fig. 4d–h) are mostly covered by vegetation and are poorly exposed. Sequences of moderately welded clast-supported lapilli and subrounded bombs are observed at the Măguricea,

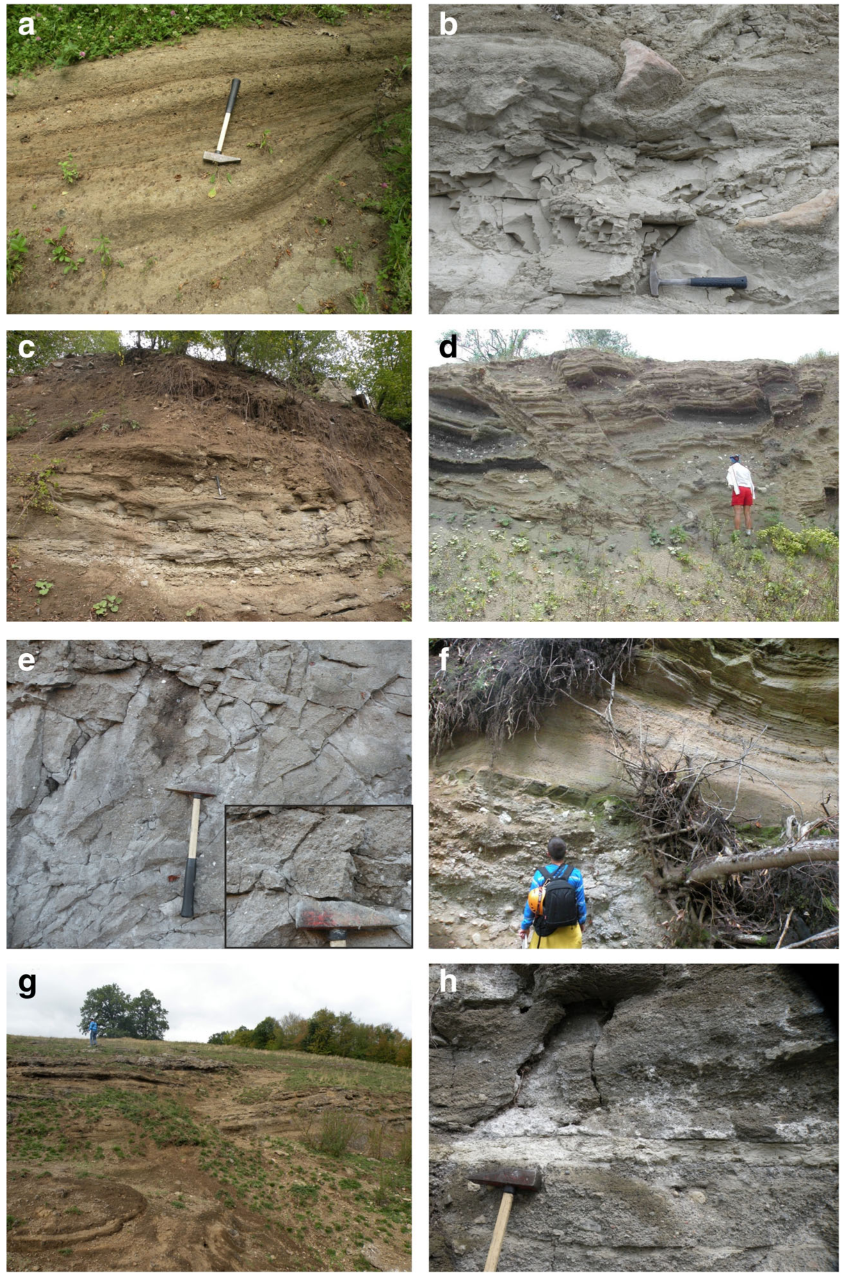

Fig. 3 PMVF phreatomagmatic deposits: **a** centimeter-decimeter-size-thick beds of pyroclastic deposits with cross-stratification (636 volcano); **b** thinly bedded pyroclastic deposits with undulatory and cross-stratification and a bomb sag (Bogata volcano); **c** centimeter-decimeter-thick pyroclastic beds with plane parallel and cross-stratification showing an alternation of fine tuffs and lapilli-tuffs rich in accidental Miocene tuff clasts and subrounded juvenile clasts (636 volcano); **d** alternation of thinly bedded and thickly bedded lapilli-tuffs rich in Miocene tuff clasts, deformed during lava flow rafting (Racoş volcano); **e** tuff-ring deposits (Bârc volcano); **f** an explosion breccia deposit overlain by a sequence of centimeter-decimeter-thick beds of ash and lapilli-tuff at the Dîlma-West volcano; **g** Eroded outer margin of a maar, showing large cross-bedded structures emplaced by base-surge currents (Bârc volcano); **h** Eroded outer margin of a tuff ring showing a large-scale cross-stratified lapilli-tuffs (Sărata volcano)

Trestia-W, Gruiu, and Gruiu-Mic volcanoes. Scoria bombs up to 1.8 m in diameter occur in the Trestia valley, and they are related to Trestia volcanoes. They are typically vesiculated in the central part, suggestive of post-ejection bubble growth. Accidental clasts of Miocene rhyolitic tuffs fragments are present in the Strombolian deposits but are less common than in the phreatomagmatic deposits.

Effusive activity

Lava flows are recorded at 18 volcanoes and are absent at the Trestia-S, Trestia-E, and Fântâna volcanoes. At the Sărata volcano, only sills and dykes are observed. Turzun, Gruiu, Pietrele, 636, Trestia-N, Comana, and Comana-S volcanoes exhibit channelized lava flows that were confined by topography. The Bârc volcano has a lava lake in the central part of the crater that ultimately breached the surrounding maar and generated a channeled flow. At other volcanoes, the lavas spread over wider areas and in some cases built up small plateaus (e.g., Gruiu-Mic, 0.35 km^2; Trestia-W volcanoes, 0.45 km^2; and the northern and western flows of Dîlma-West volcano, 0.31 km^2). The largest lava plateau (8.41 km^2) belongs to the Măguricea volcano, a typical small-sized shield volcano. Intrusions are exposed in quarries in the

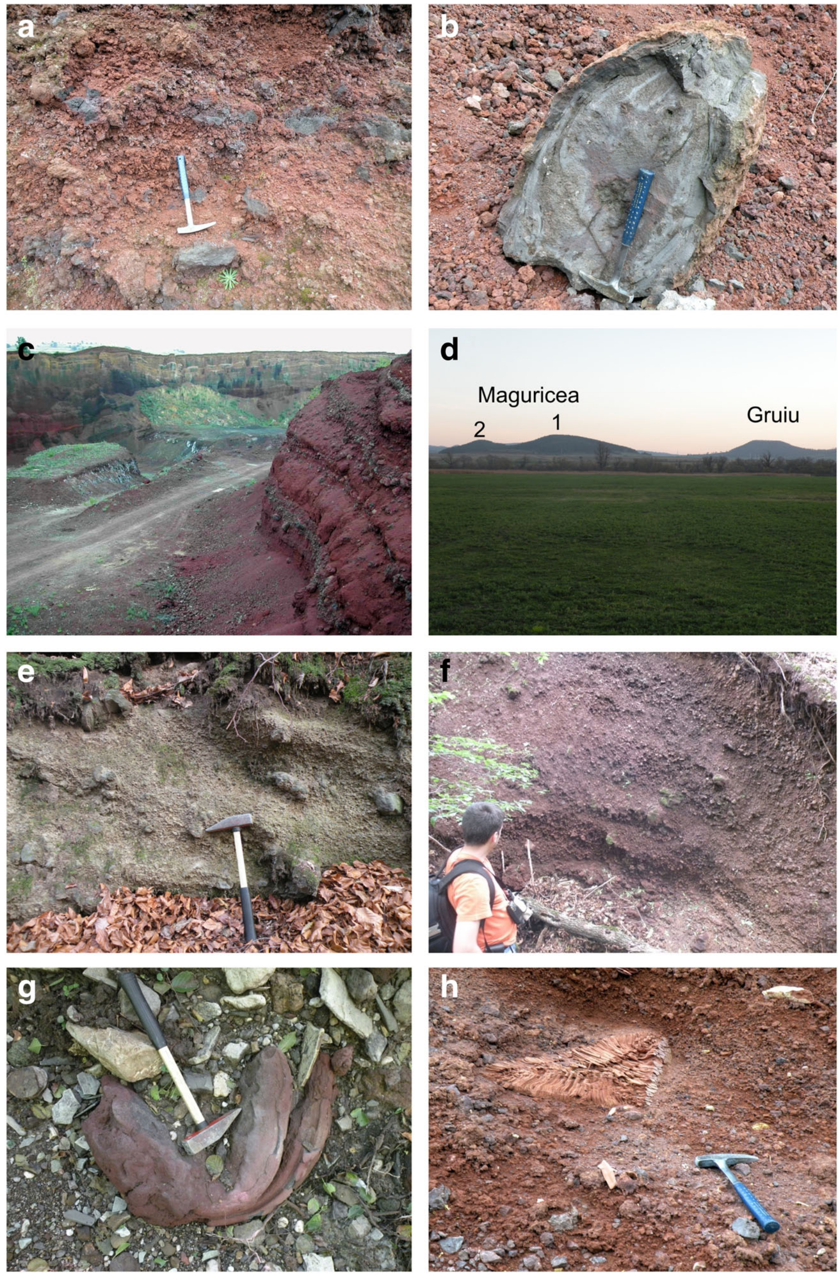

Fig. 4 PMVF Strombolian deposits: **a** welded spatter deposit containing agglutinated lapilli and bombs with fiamme-like textures (Racoş volcano); **b** meter-size fusiform bomb showing vesiculated interior and glassy outer shell (Racoş volcano); **c** view of the Hegheş quarry (Racoş) with a succession of layered and agglutinated lapilli and bomb deposits on the right-hand side and non-welded loose lapilli deposits in the background (Racoş volcano); **d** Măguricea and Gruiu scoria cones, viewed from the north; **e** agglutinated lapilli and bomb deposits emplaced in proximal facies (Pietrele volcano); **f** oblique sequence of agglutinated lapilli with rare bombs (Gruiu-Mic volcano); **g** Meter-size strongly contorted ribbon bomb found on the Trestia valley (probably from Trestia-West volcano); **h** Large rhyolitic Miocene tuff accidental clast in a lapilli-bomb agglutinated breccia; it shows polygonal cooling cracks at its margins (Racoş volcano)

Racoş volcano and at Sărata and Bogata volcanoes, where the lava flows can be traced back to sills.

The lavas typically exhibit basal and upper clinker breccia. Columnar joints are well exposed in lavas at the Racoş, Bârc, 636, Mateiaş, and Comana-S volcanoes (Fig. 5). In most cases, the lavas are dense or slightly vesiculated, and they sometimes, peripherally, show "sunburn," texture (e.g., Mihăilă and Peltz 1977), suggesting post-emplacement hydration during cooling. It consists of isometric mosaic-like "spots" of millimeter-sized patches of lighter and darker gray colored groundmass. This is thought to result from late-stage magmatic processes and non-uniform crystallization of the residual melt (White 1996; Zagożdżon 2003).

Tectonic features

The local tectonic regime is characterized by a set of inherited NW-SE-oriented normal faults that dip towards the NE and by a dominant system of NE-SW and ENE-WSW normal faults (Popescu 1970; Popescu et al. 1976). The NE-SW system generates a number of graben-like depressions along the pre-existing fractures near-parallel to the maximum principal stress (σ1). The

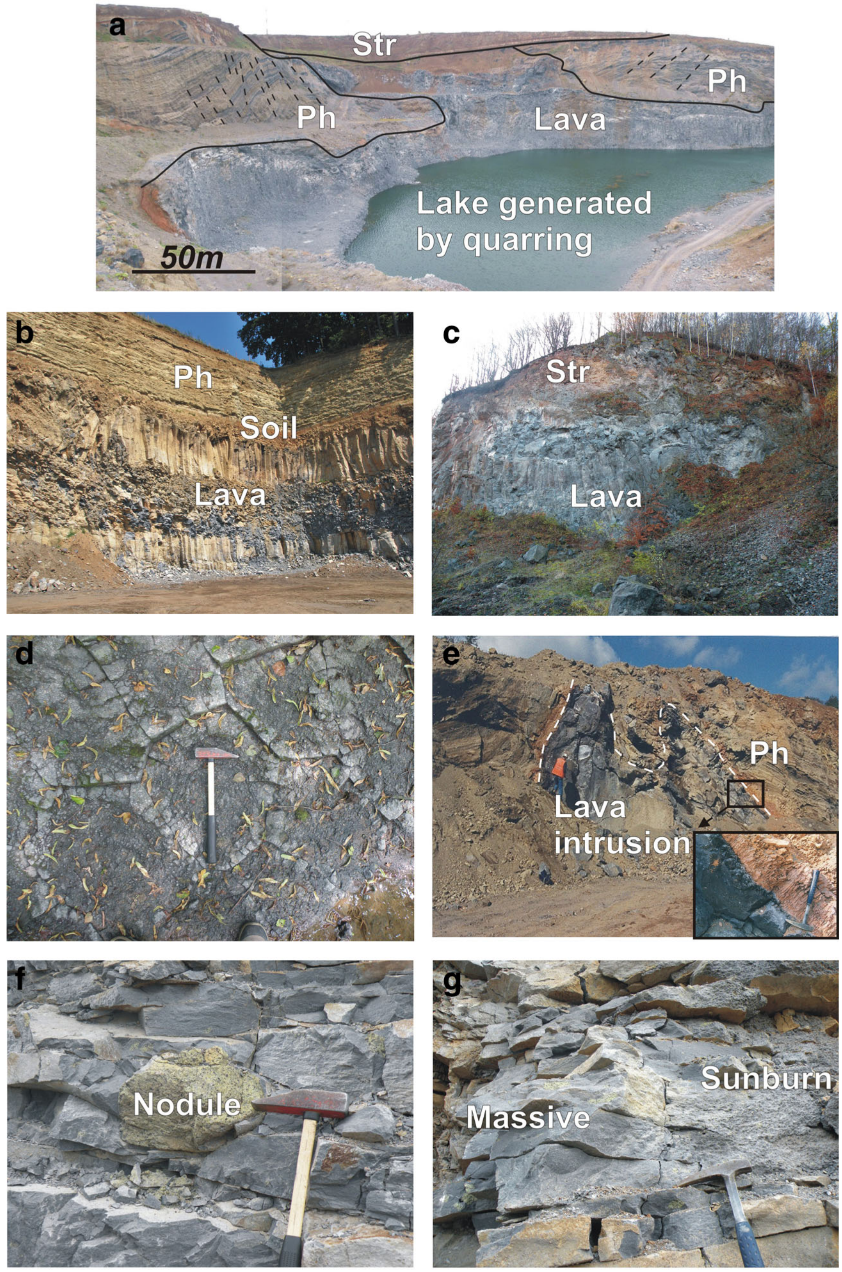

Fig. 5 PMVF lava flows: **a** relationships between the initial layered phreatomagmatic deposits, Strombolian cone deposits, sills and lava flows (Racoş volcano); **b** basaltic lava showing columnar jointing at base and top of the flow unit and subhorizontal flow-banding in the central part, covered by soil and phreatomagmatic deposits (lava of 636 volcano and pyroclastic deposits of Bogata volcano); **c** columnar jointing in a lava flow which extruded from the base of the Strombolian cone (Comana-N volcano); **d** quasi-symmetrical meter-size polygonal columnar jointing of the lavas in the central part of a solidified lava lake (Bârc volcano); **e** baked decimeter-size blocks of argillic material intercalated in the phreatomagmatic deposits and showing polygonal columnar jointing. Such material is found at the contact with vertical "finger-like" intrusions of basalt (Racoş volcano; Fig. 10); **f** lava flow with subhorizontal joints and a 30-cm mantle xenolith (Măguricea volcano); **g** transition from normal to "sunburn" lava, subhorizontal jointing (Măguricea volcano). Abbreviations: *Ph* phreatomagmatic deposits, *Str* Strombolian deposits

PMVF is largely oriented along the NE-SW trend. Observation of the fault systems inside the main volcanic area is obscured by Quaternary weathering processes and fluvial erosion. Thus, our evaluations of the current fault systems are based on recognizing the alignments of the main morphostructural elements (scarp features, river valleys). The tectonic features presented here consist of faults recognized in the basement rocks on previous maps (Popescu 1970; Popescu et al. 1976), faults recognized from morphology, and their infer extents (Fig. 6). Topography features such as continuous scarps, abrupt topographic offsets, river stream offsets (e.g., Tibaldi and Marioto 2015) or rectilinear valley segments were taken into account and interpreted as result of fault movements. One of these features is revealed at the upper reaches of Bogata valley and shows a sharp linear angle drainage deflection from NW-SE to NE-SW direction (Figs. 2 and 6). The continuous exposure of sharply truncated lava flow instead of the usual lobe-like terminations is further proof. These observations, correlated with the distribution of basement faults are the reason to consider that the sharp escarpment is a tectonic feature of an NE-SW elongated depression (deepest graben structure of the PMFV) (Figs. 2 and 6). River stream

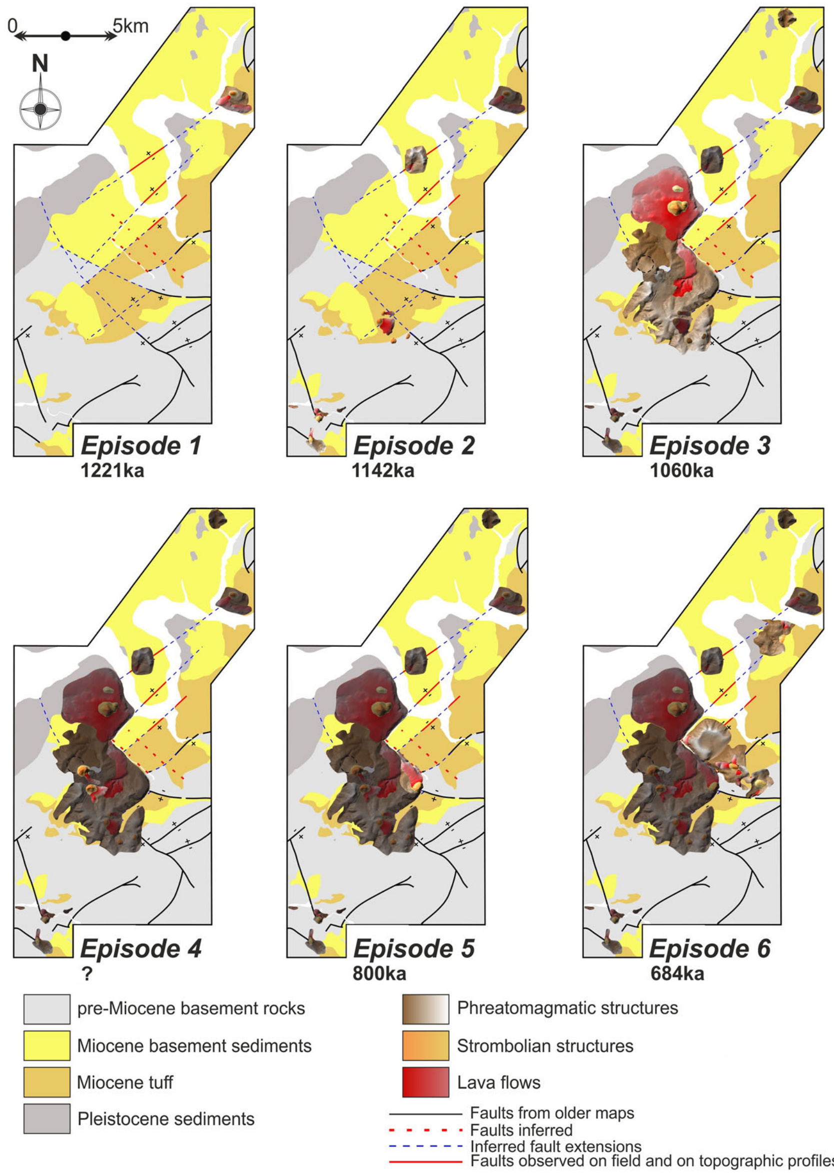

Fig. 6 Interpretative tectonic map of the PMVF with overlays of 3D volcano reconstructions, representing the six eruptive episodes. The 3D reconstructions are based on the DEMs that reflect erosion (DEMs for volume calculations eliminate the effect of erosion). *Shaded volcanic structures* are those generated during the previous eruptive episodes. Basement after Popescu (1970) and Popescu et al. (1976). Quaternary deposits (*white*) show the location of present valleys. During episode III, the deposits of the four Trestia volcanoes (3–6 in Table 1) were partly covered by a thin phreatomagmatic blanket belonging to the Bârc structure and are now mostly eroded

offsets are obvious along the Olt valley, near Turzun volcano, suggesting the presence of NE-SW faults (Fig. 2). One of these faults, whose deflected direction is indicated by a stream, broke and destroyed the lavas and Strombolian deposits of Turzun volcano, but does not disturbed the deposits of the nearby Măguricea volcano. This allows us to infer that the NE-SW fault system was active during the periods of volcanic activity.

The obvious alignment of Măguricea, Bogata, Dîlma-West, and Pietrele volcanoes coincides with the NW-SE fault system and is almost perpendicular to the main NE-SW trend. The NW-SE system is observed in another volcanic edifice alignment: Fântâna-Gruiu-Gruiu-Mic-Bârc-Trestia. On the other hand, the position of Trestia-W, Trestia-N, 636, and Dîlma-West describe the main NE-SW trend. According to Fig. 6, most volcanoes have developed in the proximity of fault intersections.

Volume calculations for lava and scoria deposits

Data used to calculate the volumes of the volcanoes and their deposits are given in Table 1, and the methodology is shown in Appendix 1.

To gain a visual representation of morphology-confined vs.morphology-unconfined lava flows, the equivalent of the mean thickness of lava flows versus their planar surface area has been plotted (Fig. 7a). The volcanoes plot in four groups. In the first group are lava flows that show a wide range of volumes and that cover a short range of planar surfaces. These

Table 1 List of the PMVF volcanic edifices, their magnetic polarity, and available $^{40}Ar/^{39}Ar$ ages

$^{40}Ar/^{39}Ar$ age polarity chron		Volcano	Volcanic structures	Volumes (without DRE correction) m^3		Surface (planar) m^2	
				Strombolian cones	Lava flows	Strombolian cones	Lava flows
1221 ka intermediate Cobb Mountain	1	Racoș[a]	PhLS	1,960,700	508,520 [FL]	122,410	229,245 [FL]
					9,448,770 [IN]		787,400 [IN]
					9,957,290 total		1,016,645 total
1142 ka reversed-polarity Matuyama	2	Turzun	PhLS	Strongly eroded	554,310	Strongly eroded	61,590
	3	Trestia-N	SL	493,130	219,490	44,900	97,000
	4	Trestia-W	SL	1,818,000	1,429,490	95,810	450,690
	5	Trestia-E	S	328,600	N/A	40,980	N/A
	6	Trestia-S	S	1,154,960	N/A	83,400	N/A
	7	Comana[a]	PhSL	2,434,540	1,353,230	85,280	118,630
	8	Comana-W	PhL	N/A	26,000	N/A	7670
	9	Comana-E	PhL	N/A	51,170	N/A	19,300
	10	Comana-S	PhSL	1,581,000	567,160	69,910	110,040
1062–1060 ka normal-polarity Jaramillo	11	Sărata	PhSL	703,440	39,620	38,880	9900
	12	Măguricea	PhSH	12,425,450 2,294,830	220,382,410	438,830 95,700	8,405,000
				1,200,030		138,180	
				15,920,310 total		672,710 total	
	13	Bârc[a]	PhL	N/A	29,653,920	N/A	1,737,720
	14	Fântâna	Ph	N/A	N/A	N/A	N/A
Unknown polarity	15	Gruiu	SL	8,911,160	1,583,260	277,560	166,940
	16	Gruiu-Mic	SL	4,990,290	1,612,710	203,040	348,260
800 ka reversed-polarity Matuyama II	17	636[a]	PhLS	4,819,330	15,219,000	208,880	874,360
684–683 ka normal-polarity Brunhes	18	Mateiaș[a]	PhSL	1,443,030	1,556,900	102,430	114,440
	19	Bogata	PhL	N/A	4,248,650	N/A	283,100
	20	Dîlma-West	PhSL	3,455,100	484,470 [N]	129,660	91,380 [N]
					416,640 [S]		187,230 [S]
					1,648,070 [W]		223,520 [W]
					2,549,110 total		502,130 total
	21	Pietrele[a]	PhSL	4,562,290	1,048,650	172,210	69,910

Volumes and surfaces covered by lava and scoria deposits are also calculated

Ph phreatomagmatic, *S* Strombolian, *L* lava, *IP* intermediate (polarity), *RP* reverse (polarity), *NP* normal (polarity), *DRE* dense rock equivalent, *FL* flow, *IN* intruded, *N* north (flow directions (in case of multiple flows)), *S* south (flow directions (in case of multiple flows)), *W* west (flow directions (in case of multiple flows))

[a] Volcanoes that are dated

lava flows have been confined by topography. The second group is defined by the products of three volcanoes (Trestia-W, Gruiu-Mic and Dîlma-West volcanoes) with lava volumes similar to those of the first group, but spread over greater planar surfaces. The southern flow of the Dîlma-West volcano was channelized, while the western and northern flows are spread across a wider area. The Racoș volcano exhibits extensive sills (their volumes have also been calculated based on outcrop occurrences and added to those of lavas). The third and fourth groups are represented by volcanoes that formed during larger volume eruptions. The third group coincides with volcanoes that have produced confined (636 volcano), or at least partly confined (Bârc volcano) lava flows. The fourth group is represented by the solitary Măguricea shield volcano, whose lava volume is one order of magnitude greater and it covers an area 4.8 times greater than that of Bârc volcano.

A rapid way to check for morphological degradation in volcanic cones is to plot the ratio of volume per planar surface, against their planar surface (Fig. 7b). We would expect that eroded (laterally spread) cones would cover a bigger planar surface, so the ratio should decrease. The data shows a large

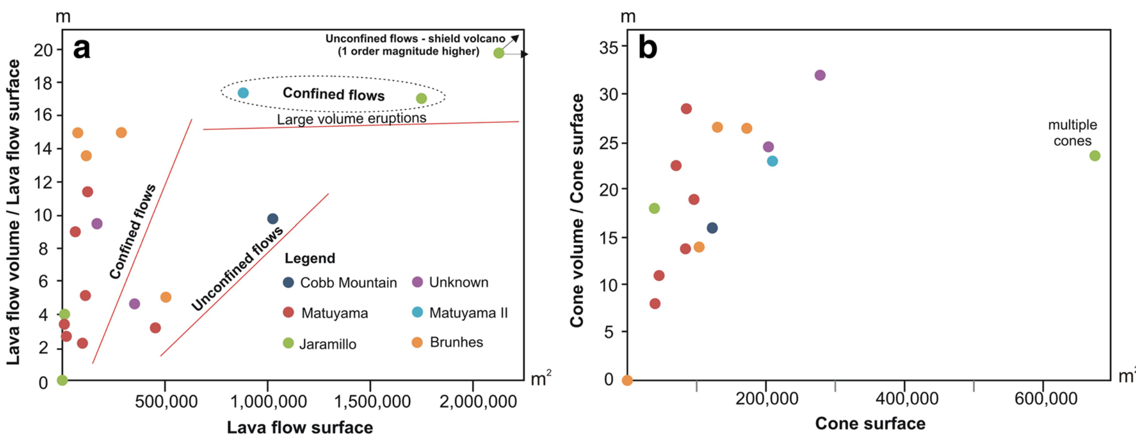

Fig. 7 Calculated volumes of lava flows and scoria deposits; **a** visual representation of confined lava flows, spread lava flows, and shield volcanoes; **b** basic representation of the degradation of cone morphology (*colors* stand for paleomagnetic ages and are the same as in (**a**))

spread, as cones generated in the same eruptive phase (Matuyama for example) cover similar planar surfaces but have different volumes. This suggests that some deposits have spread laterally more than others, although they are of the same age. The cones of Brunhes age (684 ka) show volumes similar to those of Matuyama age (1221-800 ka), but cover larger surfaces, suggesting a higher degree of erosion, although the cones are younger. These data suggests that the age of the cones is not reflected in their degree of erosion. The Măguricea volcano appears offset from the other volcanoes, because it includes three cones and thus a greater total surface area.

Volumetrically, the largest volcanoes are Măguricea, Bârc, 636 and Racoş volcanoes. Măguricea volcano has the most voluminous lavas, the largest total volume of erupted scoria (3 cones) and also the largest scoria cone. The second most voluminous cone is that of Gruiu volcano, which is 1.8 times smaller than the largest cone of Măguricea.

Discussion

Constraints on volcanic activity from K–Ar, $^{40}Ar/^{39}Ar$ and paleomagnetic data

K–Ar and paleomagnetic data have been obtained in the PMFV since the 1980’s (Ghenea et al. 1981; Mihăilă and Kreutzer 1981). The first regional attempt to combine K–Ar ages and paleomagnetic data postulated two phases of volcanic activity: The first between 1.5–1.2 Ma and the second between 0.67 and 0.52 Ma (Panaiotu et al. 2004). More accurate $^{40}Ar/^{39}Ar$ ages (Panaiotu et al. 2013) allowed the subdivision of volcanic activity into at least five episodes between 1.2 and 0.6 Ma (Figs. 2 and 8), in agreement with paleomagnetic data (Fig. 8). Some volcanoes remain undated (see Table 1) and some lack paleomagnetic data (e.g., the Gruiu and Gruiu-Mic volcanoes).

(i) According to the $^{40}Ar/^{39}Ar$ ages, the oldest volcano is the solitary Racoş volcano at 1221 ± 11 ka. This compares well with earlier K–Ar dates of 1.21 ± 0.12 Ma (Panaiotu et al. 2004) and 1.23 Ma (Mihăilă and Kreutzer 1981). All paleomagnetic directions measured at this volcano are transitional and show short period construction (Hambach et al. 1994; Panaiotu et al. 2004; Fig. 8). It corresponds to the base of the Cobb Mtn. subchron in the Geomagnetic Instability Time Scale (GITS) (Singer 2013).

(ii) The next oldest volcanic products with an age of 1142 ± 41 ka are the lava flow of Comana volcano (Fig. 2; Table 1). Five more volcanoes were identified here (three Comana, four Trestia volcanoes, and Turzun volcano), showing the same reversed polarity (Figs. 2 and 9).

(iii) Two lava flows of the Bârc volcano yield the same ages: 1062 ± 24 and 1060 ± 10 ka. They show normal polarity

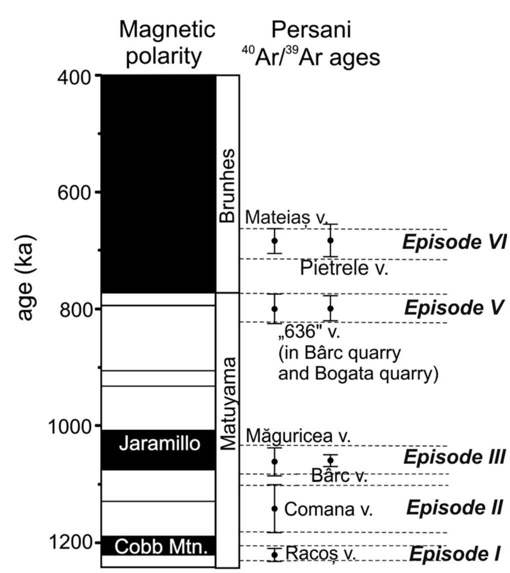

Fig. 8 Magnetic polarity time scale after Singer (2013) and $^{40}Ar/^{39}Ar$ isochron ages of PMVF basalts (Panaiotu et al. 2013)

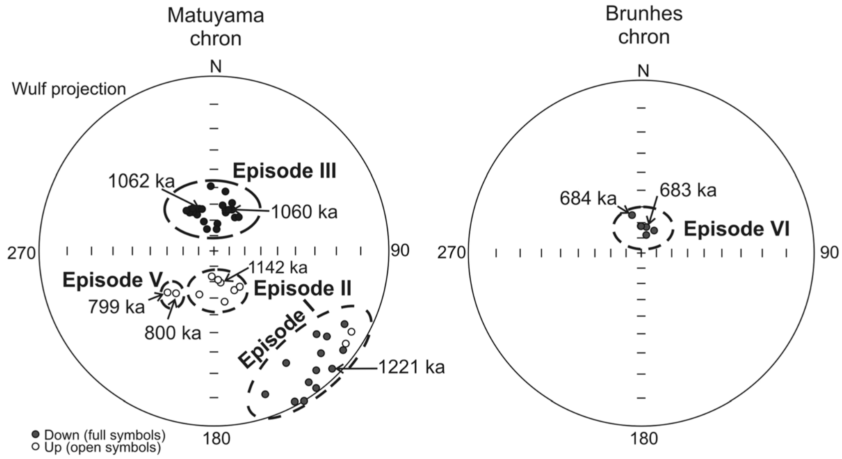

Fig. 9 Wulf projections of site-mean paleomagnetic directions from the PMVF basalts (Panaiotu et al. 2013; Panaiotu et al. 2016). *Full and open symbols* represent the lower hemisphere and upper hemispheres, respectively

and were erupted following an 80-ky period of quiescence, indicating the beginning of the Jaramillo normal subchron (e.g., Channell et al. 2010). The Măguricea, Bârc, and Sărata volcanoes were also erupted during this period, corresponding to the same subchron (Fig. 9).

(iv) Two samples from 636 volcano yielded very similar $^{40}Ar/^{39}Ar$ plateau ages of 800 ± 25 and 799 ± 21 ka, respectively (Panaiotu et al. 2013). These are substantially older than the K–Ar ages of 578 and 679 ka (Panaiotu et al. 2004), but similar to the 0.82–0.83-Ma K–Ar age suggested by Mihăilă and Kreutzer (1981). The reversed polarity of these lavas is attributed to the Matuyama II chron (Figs. 2 and 9).

(v) Lavas at the Mateiaş and Pietrele volcanoes show normal polarity and were dated at ~684 ka (684 ± 21 and 683 ± 28 ka, respectively; Fig. 2). This correlates with the Brunhes normal chron, also measured in the Bogata and Dîlma-West volcanoes (Panaiotu et al. 2016) (Fig. 9). The K–Ar eruption ages are similar (668 ± 80 ka) for Pietrele volcano (Panaiotu et al. 2004).

The gaps in the volcanic activity between the last three volcanic events (their deposits overlap in the central part of the PMVF) are supported by the presence of paleosols between volcanic deposits (e.g., Ghenea et al. 1981; Seghedi and Szakács 1994; Panaiotu et al. 2004).

Fault systems and tectonic activity

Tectonic activity associated with volcanism generated a series of graben-like structures along inherited NE-SW oriented normal faults. The deepest graben structure marks the convergence of lava flows from Măguricea, Bârc, 636, and Bogata volcano cluster. Except for Sărata, Comana-W, and Comana-E volcanoes, we can correlate the rest of the volcanic vents with faults. Five volcanoes directly overlie fault zones (the Turzun, Comana-S, 636, Bogata, and Dîlma-W volcanoes) whereas thirteen are located close to fault lines but always on the footwall block. This is in agreement with experiments and numerical models that show that dike propagation tends to be oriented parallel to the maximum external stress direction (e.g., Maccaferri et al. 2015; Rivalta et al. 2015). Numerical modeling and case studies indicate that the dykes in monogenetic fields tend to propagate towards the footwall block of normal faults because topographic height creates a higher load and stress regime (Maccaferri et al. 2015).

It is difficult to know whether both fault systems, almost perpendicular to each other, were active during specific periods of volcanic activity. However, some assumptions can be made. The eruption of Na-alkalic magmas implies extension, so at least one of the fault systems was contemporaneous with the eruptions corresponding to each episode. This was likely the NE-SW fault system along σ1, which cuts some of the volcanic deposits (e.g., Măguricea and Turzun volcanoes; Fig. 6). Since there are two systems of normal faults with different strike, almost perpendicular on each other, it suggests that each extensional period may correspond with a rotation of σ3 (e.g., Tibaldi et al. 2015). This situation is proposed in the main central cluster between the second and third episodes, less obvious for fourth and fifth, and obvious for fifth and sixth, as most of the volcanoes have been generated close to the intersection of faults (Fig. 6). The inherited NW-SE-oriented alignment is suggesting a NE-SW direction of σ3. It means that volcanoes with a given alignment were favored because their feeder dykes were perpendicular to σ3, whereas the other alignment was blocked since it was perpendicular to the horizontal greatest principal stress (σ1), and vice versa after rotation of σ3. It is noticeable that the paths and geometry of dyke propagation and emplacement during volcanic evolution was controlled by the specific local extension periods and block rotations between 1.2 and 0.6 Ma which may be characteristic for the post-collisional setting of PMVF.

The monogenetic character of the PMVF is most likely related to the fact that, once a volcano was emplaced, the upper part of the plumbing system was sealed by solidifying magmas that remained in the conduits (e.g., Kereszturi and Németh 2012; Valentine 2012). In the PMVF, because of the multitude of faults, the complex and variable stress regime and the interplay between σ1 and σ3, we infer that it was easier for new magma batches to find other pathways and erupt in slightly different locations rather than using the same high-level plumbing system and build polygenetic volcanoes. The volcano clustering that started in the third episode in the central area of PMVF may represent the largest volume of melt collection and extraction from the mantle source (e.g., Tadini et al. 2014).

Eruptive history

By combining published ages, paleomagnetic data with our new volcanological information, we can better understand the eruptive history of the PMVF, which consists of the following episodes (Figs. 8 and 9):

Episode I (1221 ka)

This episode was marked by the eruption of the Racoş volcano, which was characterized by initial phreatomagmatic activity followed by a Strombolian phase, and then by an effusive and minor intrusive phase (Fig. 10). The phreatomagmatic deposits containing abundant rhyolitic tuff xenoliths that suggest that explosive magma-water interaction occurred at depths of ~100–150 m, in an aquifer hosted by Miocene rhyolitic tuffs. The phreatomagmatic phase generated near-vent explosion-derived dilute pyroclastic density currents and co-PDC ash fall deposition that over time constructed a tuff ring. It was progressively enlarged by further explosions generated by roughly coeval phreatomagmatic and Strombolian activity. This probably marks the transition towards the Strombolian activity of this volcano, which generated the scoria cone (Fig. 10). Later magmas penetrated as dykes or sills and formed a lava lake in the tuff-ring crater. We infer that the scoria cone load exerted pressure on the emerging lava that, by moving centrifugally, caused the collapse of sections of the tuff ring, which were internally faulted (see Fig. 3d) and rafted away.

Episode II (~1142 ka)

This episode marks the generation of two groups of four volcanoes each (Trestia-N, Trestia-W, Trestia-E, and Trestia-S volcanoes and Comana, Comana-W, Comana-E, and Comana-S volcanoes) and by the solitary Turzun volcano. All eruptions along the Comana valley started with phreatomagmatic activity and then transitioned into magmatic eruptions. Comana and Comana-S volcanoes developed maar structures, as indicated by the present-day topography which shows that the floors of the craters were excavated in the bedrock (sensu Kereszturi and Németh 2012). This phase was followed by cone-building Strombolian eruptions and effusive activity that emitted lava flows from the base of the cinder cones. The eruption of Comana-E and Comana-W volcanoes generated EW-directed pyroclastic density currents, without excavating craters. Since the lavas are also confined to the same narrow elongated areas, we infer that these deposits were emplaced by fissure eruptions, or alternatively, were confined by topography. Strombolian activity is not recorded here, as the initial phreatomagmatic phase was closely followed by emission of lava flows.

The Trestia volcanoes (3–6 in Table 1; Fig. 2) lack phreatomagmatic activity and are characterized by cone-building Strombolian activity. Effusion of lavas is recorded at Trestia-N and Trestia-W volcanoes. Since the four Trestia edifices directly overly the Miocene tuff deposits and no evidence for magma-water interaction was observed, we infer that the aquifer was depleted or lowered. The Trestia volcanoes are partially covered by an eroded phreatomagmatic blanket erupted from the younger Bârc volcano (Figs. 2 and 7).

The eruption of Turzun volcano started with a phreatomagmatic phase that generated a tuff ring. Eruptive activity continued with a minor Strombolian phase followed

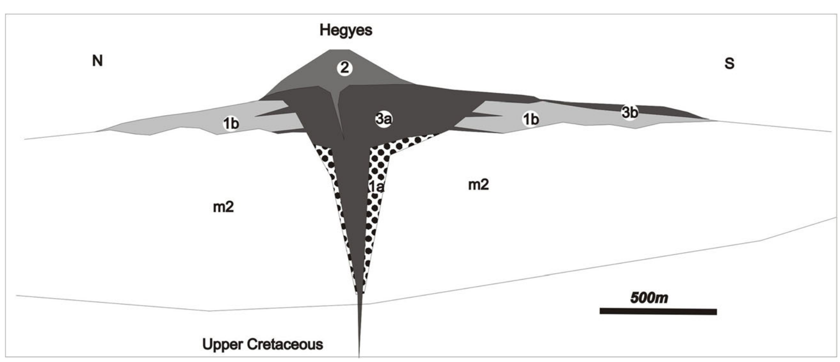

Fig. 10 Interpretative section through Racoş volcano: *1a* phreatomagmatic vent deposits; *1b* tuff-ring deposits; *2* Strombolian scoria and lapilli-tuff cone, rare lava flows; *3a* magma generating a lava lake and sills/dykes intruding the older edifice; *3b* lava flows rafting the phreatomagmatic deposits; *m2* Miocene rhyolitic tuff deposits

by effusion of lava flows that were confined in a valley created by a NE-SW normal fault system.

Episode III (~1060 ka)

This was the most intense volcanic episode in the history of the PMVF and generated the greatest volumes of scoria and lava deposits.

The eruption at Bârc volcano started with intense phreatomagmatic activity that constructed a 2.25-km-wide tuff ring that evolved into a maar (sensu Lorenz and Kurszlaukis 2007). The ensuing effusive phase filled the maar with a lava lake. Ultimately, the lavas breached the NE side of the initial tuff-ring structure and flowed northward for ~1.5 km.

The eruption of Măguricea volcano also started with a phreatomagmatic phase, followed by Strombolian activity responsible for building three cones. Lava flows breached the base of the cones and extended into several plateau-forming flow-fields characteristic for a shield volcano (Fig. 2). Two other volcanoes are attributed to this episode: Fântâna, based on volcanological observations and Sărata based on paleomagnetic and K–Ar data.

The Fântâna maar volcano was formed solely by a phreatomagmatic explosion. The pyroclastic deposits contain many conglomerate and Cretaceous limestone clasts and based on the local stratigraphy, this implies that the magma-water interaction took place at a depth of ~150 m.

The eruption of Sărata volcano started with a tuff-ring-forming phreatomagmatic event (Fig. 3h). The water-magma interaction fluctuated, as suggested by the welded Strombolian deposit in its inner-northern margin. A sill was emplaced in the base of the southern wall of the inner-crater suggest an incipient effusive activity.

Episode IV (Gruiu and Gruiu-Mic volcanoes)

There are currently no age or paleomagnetic data for the Gruiu and Gruiu-Mic volcanoes. Both developed near the Bârc volcano; Gruiu-Mic on the inner side and Gruiu on a limestone basement between the Bârc and Fântâna volcanoes (Fig. 2). Both of the volcanoes lack evidence for the initial phreatomagmatic activity and the eruptions instead were characterized by initial cone-building Strombolian activity, followed by effusion of lava from the base of the cones; this partially breached the cones. The Gruiu-Mic lava flows partially cover the lava lake of the Bârc maar, while the lava flowing from Gruiu volcano was confined between the tuff-ring structure of Bârc volcano and the cone and lavas of Gruiu-Mic volcano. We infer that the two volcanoes were constructed more or less simultaneously as they are both in close proximity and had a similar behavior. The lack of magma-water interaction may suggest that the aquifer level was depleted at the time of the eruptions. We speculate that the phreatomagmatic activity of the older Bârc volcano may have led to a temporary depletion of the aquifer, so that Gruiu-Mic and Gruiu volcanoes may have erupted before the aquifer was restored. It is also probable that missing aquifer could be associated with dry climate conditions at the time of eruption.

Episode V (800 ka)

This episode was marked by the eruption of the 636 volcano. Activity commenced with a phreatomagmatic phase (Fig. 3c) that damaged the eastern part of the Bârc volcano. This was followed by a Strombolian phase that built a cone on the southern margin of the 636 volcano and by effusion of lava that breached the base of the cone. There are no remnants of tuff-ring structures, and the floor of the crater seems to have been excavated in bedrock.

Episode VI (~684 ka)

Four volcanoes were formed during this episode: Mateiaş (isolated), Bogata, Dîlma-West, and Pietrele (aligned on a NW-SE direction) (Fig. 2).

Mateiaş volcano was developed on an inclined slope, and during the eruption, initial phreatomagmatic activity led to the building of an asymmetrical edifice (Seghedi and Szakács 1994) that resembles a tuff ring. Subsequent changes in eruptive style generated a buttressed scoria cone and a lava flow, fed by a sill that rafted away parts of the phreatomagmatic deposits.

The Bogata volcano tuff ring has deposits that are rich in accidental Miocene tuff and Cretaceous limestone ballistic bombs. It is the only volcano of this group that lacks evidence

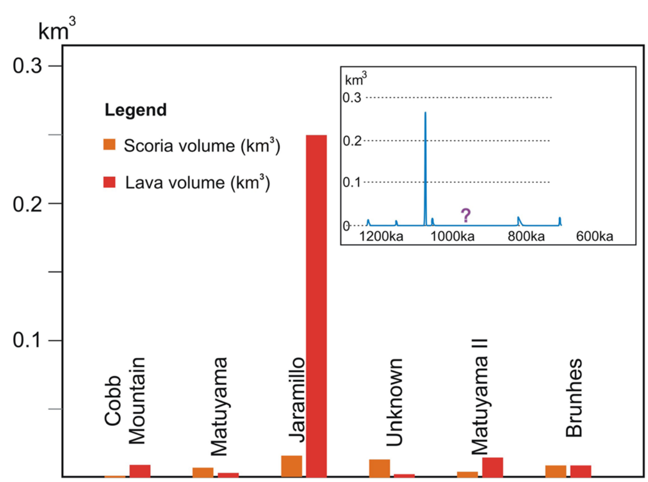

Fig. 11 Erupted volumes of scoria and lava deposits shown according to each episode of volcanic activity. The *inlet* shows the cumulative volumes (lava + scoria) and the time gaps between the eruption episodes. *Question mark* represents the uncertain age of the fourth eruptive episode. Up until the third episode (Jaramillo), the eruptions were time predictable

for Strombolian activity. A lava flow extends from a sill in the western wall of the cone.

The Dîlma-West and Pietrele volcanoes are very similar. Both eruptions started with phreatomagmatic phases that constructed a maar volcano. Both maars were subsequently filled by scoria cones and lava flows. Pietrele volcano has one lava flow that extends from a sill injection. The Dîlma-West volcano erupted three lava flows.

According to the volume data (Fig. 11), the first eruptive episode (Cobb Mountain age) shows the smallest volumes of erupted scoria, while the second episode (Matuyama) is responsible for scoria volumes that are four times greater. The largest total volumes, for both lava flows and scoria deposits are recorded in the third episode of volcanic activity (Jaramillo). The second most voluminous lava flows are recorded in the fifth episode (Matuyama II, >16.4 times less voluminous than those of Jaramillo), while the second most voluminous scoria deposits are in the fourth episode of activity (Gruiu and Gruiu-Mic, 1.2 times smaller than those of Jaramillo). In the sixth episode of volcanic activity (Brunhes), the volumes of scoria deposits and lava flows are similar; however, in the absence of the DRE correction, the calculated scoria volumes cannot be directly compared with those of the lavas, which are generally non-vesicular. By assuming a mean scoria vesicularity of 50 %, the volumes of magma erupted during the Strombolian/Hawaiian phases is reflected by half of the calculated scoria volumes. The smallest volcanoes were generated during the second episode, with Comana-W and Comana-E as the least voluminous. After the peak activity of the third episode (Măguricea and Bârc volcanoes), the three subsequent eruption episodes resulted in greater volumes of scoria deposits and lava flows than the eruptions that preceded the peak activity.

Conclusions

The PMVF is composed of 21 monogenetic volcanoes that erupted during six episodes: one volcano at around 1221 ka; nine volcanoes at 1142 ka; four volcanoes at 1060 ka (the period of most voluminous volcanism); two volcanoes shortly after (exact age unknown); one volcano at 800 ka; and four more at around 684 ka. Five of the eruptive episodes had initial phreatomagmatic eruptions (15 out of 21 volcanoes). Phreatomagmatism was usually followed by Strombolian/Hawaiian activity (at 10 out of 15 volcanoes) and then by a final effusive phase (at 14 out of 15 volcanoes). The second and fourth eruptive episodes were periods when magma-water interactions did not take place.

The PMVF developed in a period of extensional tectonism, and the locations of the volcanic centers are closely related to local fault systems and to the latter's effect on topography and stress regime. Some of the vents are located along faults, but most are located near faults (within less than ~50 m) within their footwall block. Dyke emplacement was controlled by specific local block rotations and periods of extension. It seems that it was easier for subsequent magma batches to find new pathways than to re-use the older upper-plumbing systems which were partially sealed-off by the previously solidified magmas. Developing new or complex upper-plumbing systems that allow for multiple vents is in our opinion related to the multitude of faults and to their complicated effect on the topography and on the underground stress regime, which in the end determined the monogenetic behavior of these volcanoes.

The monogenetic volcanism of the PMVF was time-predictable only up to the Jaramillo-aged eruptions. After this, the eruptions became neither time nor volume predictable. Timing of the eruptions and the volumes erupted during activity of succeeding episodes may be related to the development and intensity of crustal extension and the extent of melt extraction in the mantle source.

Acknowledgments This work was supported by a grant of the Ministry of Education and Scientific Research, CNCS-UEFISCDI, project number PN-II-IDPCE-2012-4-0137. Constructive reviews provided by Alessandro Tibaldi and Gábor Kereszturi helped to improve our manuscript. Thorough editorial handling by Richard J. Brown and James White is appreciated.

References

Channell JET, Hodell DA, Singer BS, Xuan C (2010) Reconciling astrochronological and ^{40}Ar/^{39}Ar ages for the Matuyama–Brunhes boundary and late Matuyama chron. Geochem Geophys Geosyst 11. doi:10.1029/2010GC003203Q0AA12

Cimarelli C, Di Traglia F, de Rita D, Gimeno Torrente D, Fernandez Turiel J-L (2013) Space–time evolution of monogenetic volcanism in the mafic Garrotxa volcanic field (NE Iberian Peninsula. Bull Volcanol 75:758

Connor CB, Conway FM (2000) Basaltic volcanic fields. In: Sigurdsson H, Houghton BF, McNutt SR, Rymer H, Stix J (eds) Encyclopedia of volcanoes. Academic Press, San Diego, pp. 331–343

Downes H, Seghedi I, Szakács A, Dobosi G, James DE, Vaselli O, Rigby IJ, Ingram GA, Rex D, Pécskay Z (1995) Petrology and geochemistry of the late Tertiary/Quaternary mafic alkaline volcanism in Romania. Lithos 35:65–81

Falus G, Tommasi A, Ingrin J, Szabó C (2008) Deformation and seismic anisotropy of the lithospheric mantle in the southeastern Carpathians inferred from the study of mantle xenoliths. Earth Planet Sci Lett 272:50–64

Fisher RV, Schmincke H-U (1984) Pyroclastic rocks. Springer-Verlag, Berlin, p. 472

Gaffney ES, Damjanac B, Valentine GA (2007) Localization of volcanic activity: 2. Effects of pre-existing structure. Earth Planet Sci Lett 263(3–4):323–338

Ghenea C, Bandrabur T, Mihăilă N, Rădulescu C, Samson P, Rădan S (1981) Pliocene and Pleistocene deposits in the Braşov Depression. In: Guidebook for the field excursion 1–8 June 1981, Subcommission for European Quaternary Stratigraphy. Published by the Institute of Geology and Geophysics, p. 55

Hambach U, Orleanu M, Rogenhagen J, Schnepp E (1994) Paleomagnetism of Pleistocene volcanics from the Perşani Mountains, East Carpathians (Romania). Rom J Tectonics Reg Geol 75:20–24

Harangi S, Sági T., Seghedi I, Ntaflos T (2013) A combined whole-rock and mineral-scale investigation to reveal the origin of the basaltic magmas of the Perşani monogenetic volcanic field, Romania, Eastern-Central Europe. Lithos 180–181:43–57

Harangi S, Jankovics MÉ, Sági T, Kiss B, Lukács R, Soós I (2014) Origin and geodynamic relationships of the late Miocene to Quaternary alkaline basalt volcanism in the Pannonian basin, Eastern–Central Europe. Int J Earth Sci (Geol Rundsch). doi:10.1007/s00531-014-1105-7

Hauer F, Stache G (1863) Geologie Siebenb rgens. Wilhelm Braunm ler, Wien, p. 637

Herbich Fr (1878) Das Szeklerland. Jahrb. Der Kgl. Und geol. Aust, V, Budapest

Kereszturi G, Németh K (2012) Monogenetic basaltic volcanoes: genetic classification, growth, geomorphology and degradation. In: Németh, K. (ed) Updates in volcanology—new advances in understanding volcanic systems, chapter 1, pp. 3–88

Kereszturi G, Németh K, Csillag G, Balogh K, Kovács J (2011) The role of external environmental factors in changing eruption styles of monogenetic volcanoes in a Mio/Pleistocene continental volcanic field in western Hungary. J Volcanol Geotherm Res 201(1–4):227–240

Koch A (1900) Die Tertiärbildungen des Beckens der Siebenburgischen Landesteile. Neogen teile, Budapest

Lațiu V (1928) Contribution to the petrographic study of the basalt with quartz xenolith from Racoşul de Jos. An Inst Geol Rom XIII:1–22, Bucharest (In Romanian)

Le Corvec N, Spörli KB, Rowland J, Lindsay J (2013) Spatial distributionand alignments of volcanic centers: clues to the formation of monogenetic volcanic fields. Earth-Sci Rev 124:96–114

Lexa J, Seghedi I, Németh K, Szakács A, Konečný V, Pécskay Z, et al. (2010) Neogene-Quaternary volcanic forms in the Carpathian-Pannonian Region: a review. Cent Eur. J Geosci 2(3):207–270

Lorenz V, Kurszlaukis S (2007) Root zone processes in the phreatomagmatic pipe emplacement model and consequences for the evolution of maar–diatreme volcanoes. J Volcanol Geotherm Res 159:4–32

Lustrino M, Wilson M (2007) The circum-Mediterranean anorogenic Cenozoic igneous province. Earth Sci Rev 81:1–65

Maccaferri F, Acocella V, Rivalta E (2015) How differential load induced by normal fault scarps controls the distribution of monogenetic volcanism. Geophys Res Lett. doi:10.1002/2015GL065638

Martí J, Planaguma L, Geyer A, Canal E, Pedrazzi D (2011) Complex interaction between Strombolian and phreatomagmatic eruptions in the Quaternary monogenetic volcanism of the Catalan Volcanic Zone (NE of Spain. J Volcanol Geotherm Res 201(1–4):178–193

Martin U, Németh K (2004) Mio-Pliocene phreatomagmatic volcanism in the Western Pannonian Basin. Budapest, Geological Institute of Hungary, p. 193

Matenco L, Bertotti G, Leever K, Cloetingh S, Schmid SM, Tărăpoancă M, Dinu C (2007) Large-scale deformation in a locked collisional boundary: interplay between subsidence and uplift, intraplate stress, and inherited lithospheric structure in the late stage of the SE Carpathians evolution. Tectonics 26 . doi:10.1029/2006TC001951 TC4011

Matenco L, Krézsek C, Merten S, Schmid S, Cloetingh S, Andriessen P (2010) Characteristics of collisional orogens with low topographic build-up: an example from the Carpathians. Terra Nov. 22:155–165

Mihăilă N, Kreuzer H (1981) Contribution to the knowledge of basaltic volcanics from Perşani. Terra 4:37–47 (in Romanian)

Mihăilă N, Peltz S (1977) Contribution to the knowledge of Heghies volcano (Racoşul de Jos—Munții Perşani). DS Inst Geol LXIII 5: 60–83 Bucharest (in Romanian)

Mihăilă N, Peltz S, Wonner F (1972) New data concerning the Quaternary deposits and basaltic volcanism from the Hoghiz-Veneția. St Tehn Ec, H4:69–93, Bucharest (In Romanian)

Németh K (2012) An overview of the monogenetic volcanic fields of the Western Pannonian Basin: their field characteristics and outlook for future research from a global perspective. In: Stoppa F (ed) Updates in volcanology—a comprehensive approach to volcanological problems. In-Tech:27–52

Németh K, Martin U (1999) Late Miocene paleo-geomorphology of the Bakony-Balaton Highland Volcanic Field (Hungary) using physical volcanology data. Z Geomorphol 43(4):417–438

Németh K, Martin U (2007) Shallow sill and dyke complex in western Hungary as a possible feeding system of phreatomagmatic volcanoes in "soft-rock" environment. J Volcanol Geotherm Res 159(1–3):138–152

Panaiotu CG, Pécskay Z, Hambach U, Seghedi I, Panaiotu CC, Itaya CET, Orleanu M, Szakács A (2004) Short-lived Quaternary volcanism in the Perşani Mountains (Romania) revealed by combined K–Ar and paleomagnetic data. Geol Carpathica 55:333–339

Panaiotu CG, Vişan M, Țugui A, Seghedi I, Panaiotu AG (2013) Palaeomagnetism of the South Harghita volcanic rocks of the East Carpathians: implications for tectonic rotations and palaeosecular variation in the past 5 Ma. Geophys J Int 189:369–382

Panaiotu CG, Dimofte D, Necula C, Dumitru A, Seghedi I, Popa R-G (2016) Revised paleosecular variation from Quaternary lava flows from the east Carpathians. Romania. Reports in Physics 68(1):416–424

Popescu I (1970) Geological map 1:50000, sheet Perşani 94b, L-35-75b, Geological Institute of Romania

Popescu I, Mihăilă N, Peltz S, Țicleanu N, Andreescu I (1976) Geological map 1:50000, sheet Racoş 78d, L-35-63d, Geological Institute of Romania

Preda D (1940). Les basaltes du versant du oust de Monts Perşani. DS Inst Geol Roum XXIV: 90–98, Bucharest

Rivalta E, Taisne B, Bunger AP, Katz RF (2015) A review of mechanical models of dike propagation: schools of thought, results and future directions. Tectonophysics 638:1–42

Săndulescu M (1984) Geotectonics of Romania. Ed Tehnică, Bucureşti, p. 366 (in Romanian)

Schmid S, Bernoulli D, Fügenschuh B, Matenco L, Schefer S, Schuster R, Tischler M, Ustaszewski K (2008) The Alpine–Carpathian–Dinaridic orogenic system: correlation and evolution of tectonic units. Swiss J Geosci 101:139–183

Seghedi I, Szakács A (1994) Upper Pliocene to Quaternary basaltic volcanism in the Perşani Mountains, Romania. Rom. J Petrol 76:101–107

Seghedi I, Downes H, Szakács A, Mason PRD, Thirlwall MF, Roşu E, Pécskay Z, Marton E, Panaiotu C (2004) Neogene-Quaternary magmatism and geodynamics in the Carpathian–Pannonian region: a synthesis. Lithos 72:117–146

Seghedi I, Matenco L, Downes H, Mason PRD, Szakács A, Pécskay Z (2011) Tectonic significance of changes in post-subduction Pliocene-Quaternary magmatism in the south east part of the Carpathian–Pannonian region. Tectonophysics 502:146–157

Singer BS (2013) A Quaternary geomagnetic instability time scale. Quat Geochronol 21:29–52

Szakács A, Seghedi I, Pécskay Z (1993) Pecularities of South Harghita Mts. as terminal segment of the Carpathian Neogene to Quaternary volcanic chain. Rev Roum de Géol 37:21–36

Tadini A, Bonali FL, Corazzato C, Cortés JA, Tibaldi A, Valentine GA (2014) Spatial distribution and structural analysis of vents in the Lunar Crater Volcanic Field (Nevada, USA. Bull Volcanol 76:877. doi:10.1007/s00445-014-0877-8

Tibaldi A, Mariotto FP (2015) Structural geology of active tectonic areas and volcanic regions. Lulu Press, Inc, p. 203
Valentine GA (2012) Shallow plumbing systems for small-volume basaltic volcanoes, 2: evidence from crustal xenoliths at scoria cones and maars. J Volcanol Geotherm Res:223–224 47–63
Valentine GA, Gregg TKP (2008) Continental basaltic volcanoes-processes and problems. J Volcanol Geotherm Res 177:857–873
Valentine G, Perry F (2007) Tectonically controlled, time-predictable basaltic volcanism from lithospheric mantle source. Earth Planet Sci Lett 261:201–216
Vaselli O, Downes H, Thirlwall MF, Dobosi G, Coradossi N, Seghedi I, Szakács A, Vannucci R (1995) Ultramafic xenoliths in Plio-Pleistocene alkali basalts from the Eastern Transylvanian basin: depleted mantle enriched by vein metasomatism. J Petrol 36:23–55
Vergniolle S, Mangan M (2000) Hawaiian and Strombolian eruptions. In: Sigurdsson H, Houghton B, McNutt S, Rymer H, Stix J (eds) Encyclopedia of volcanoes. Academic Press, New York, pp. 447–461
Wachner H (1915) Bericht uber die im Sommer des Jahre 1915 im Persani Gebirge ausgefuhrten geologichen Aufnauhmen. Jahresber D.K. und Geol. D.K., pp. 268–285
White JDL (1996) Impure coolants and interaction dynamics of phreatomagmatic eruptions. J Volcanol Geotherm Res 74:15.5–1170
White JDL, Houghton BF (2006) Primary volcaniclastic rocks. Geology 34(8):677–680
Zagożdżon PP (2003) Sunburn in the tertiary basalts of Silesia (SW Poland). Geolines 15:188–193